New method for real-time visualization and quantitative characterization of early colorectal cancer in endoscopy: a pilot study

OPEN ACCESS

Authors

Andrej Wagner[1], Stephan Zandanell[1], Alexander Ziachehabi[2], Alexander Mitrakov[3], Eckhard Klieser[4], Daniel Neureiter[4], Tobias Kiesslich[1,5], Christian Mayr[5], Frieder Berr[1], Michael Fedoruk[6], Franz Singhartinger[7], Josef Holzinger[7]

Institutions

1 Department of Internal Medicine I, University Clinics Salzburg, Paracelsus Medical University, Salzburg, Austria
2 Department of Medicine II, Kepler Medical University, Linz, Austria
3 Endoscopy Division, Nizhniy Novgorod Cancer Hospital, Nizhniy Novgorod, Russian Federation
4 Institute of Pathology, Paracelsus Medical University/ Salzburger Landeskliniken (SALK), Salzburg, Austria
5 Laboratory for Tumour Biology and Experimental Therapies (TREAT), Institute of Physiology and Pathophysiology, Paracelsus Medical University, Salzburg, Austria
6 Vortex Photonics, Planegg, Germany
7 Department of Surgery, University Clinics Salzburg, Paracelsus Medical University, Salzburg, Austria

submitted 31.8.2021
accepted after revision 9.5.2022
published online 9.5.2022

Bibliography
Endosc Int Open 2022; 10: E1147–E1154
DOI 10.1055/a-1847-2820
ISSN 2364-3722

Georg Thieme Verlag KG, Rüdigerstraße 14, 70469 Stuttgart, Germany

Corresponding author
Andrej Wagner, MD, Department of Internal Medicine I, University Clinics Salzburg, Paracelsus Medical University, Müllner Hauptstrasse 48, 5020 Salzburg, Austria
Fax: +43 5 7255 25599
and.wagner@salk.at

Supplementary material is available under https://doi.org/10.1055/a-1847-2820

ABSTRACT

Background and study aims Endoscopic optical diagnosis is crucial to the therapeutic strategy for early gastrointestinal cancer. It accurately (>85%) predicts pT category based on microsurface (SP) and vascular patterns (VP). However, interobserver variability is a major problem. We have visualized and digitalized the graded irregularities based on bioinformatically enhanced quantitative endoscopic image analysis (BEE) of high-definition white-light images.

Methods In a pilot study of 26 large colorectal lesions (LCLs, mean diameter 39 mm), we retrospectively compared BEE variables with corresponding histopathology of the resected LCLs.

Results We included 10 adenomas with low-grade intraepithelial neoplasia (LGIN), nine with high-grade intraepithelial neoplasia (HGIN) and early adenocarcinoma (EAC), and seven deeply submucosal invasive carcinomas. Quantified density (d) and nonuniformity (C_U) of vascular and surface structures correlated with histology (r_s d VP: –0.77, r_s C_U VP: 0.13, r_s d SP: –0.76, and r_s C_U SP: 0.45, respectively). A computed BEE score showed a sensitivity and specificity of 90% and 100% in the group with LGINs, 89% and 41% in the group with HGINs and EACs, and 100% and 95% in the group with deeply invasive carcinoma, respectively.

Conclusions In this pilot study, BEE showed promise as a tool for endoscopic characterization of LCLs during routine endoscopy. Prospective clinical studies are needed.

	JNET 2A	JNET 2B	JNET 3
Vessel pattern	Regular caliber, distribution (meshed/spiral pattern)	Variable caliber, irregular distribution	Loose vessel areas, interruption of thick vessels
Surface pattern	Regular (tubular/branched/papillary)	Irregular or obscure	Amorphous areas
Endoscopic image		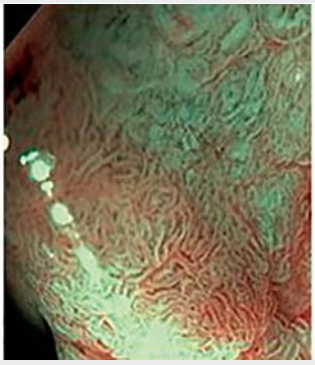	
Most likely histology	Adenoma with LGIN	Adenoma with HGIN or early carcinoma with <sm2	Submucosal deeply invasive carcinoma ≥sm2
Curative treatment	EMR or PM-EMR	En-bloc EMR or ESD	Surgical oncological resection

▶ **Fig. 1** JNET classification criteria and treatment options (according to [4, 5]). Abbreviations: JNET: Japan NBI expert team classification, LGIN: low-grade intraepithelial neoplasia, HGIN: high-grade intraepithelial neoplasia, sm2: submucosal invasion > 1000 µm, EMR: endoscopic mucosal resection, PM: piecemeal, ESD: endoscopic submucosal dissection.

Introduction

Accurate endoscopic assessment of the malignant potential and depth of invasion of colorectal neoplasms is crucially important for patients. This is the only way to select the indicated resection procedure (endoscopic resection, en-bloc or piecemeal, or oncologic surgical resection). The established contrast-enhancing endoscopy and magnification techniques allow statistically reliable in situ differentiation of malignant and non-malignant lesions in patients and prediction of the depth of submucosal invasion [1]. In colorectal cancer, randomized trials and meta-analyses suggest a statistical accuracy of over 85 % [2, 3]. The Japan NBI Expert Team classification of colorectal neoplasia (JNET, [4, 5]) differentiates between colorectal lesions suitable for endoscopic (en-bloc) resection and candidates for surgical oncological therapy (▶ **Fig. 1**).

Unfortunately, optical characterization of large colorectal lesions (LCLs) is suboptimal in daily clinical practice, because interobserver variation is too great for accurate prediction of the pT category of the neoplasia. In a recently published study [6], only 39 % of all T1 colon carcinomas were correctly characterized. Correct diagnostic assessment of LCLs may prevent inadequate endoscopic piecemeal resections resulting in unnecessary surgical procedures.

Bioinformatically enhanced endoscopy (BEE) is a novel tool for visualization and quantitative analysis of microstructures on routine high-definition endoscopic white-light images (HD-WLE, ▶ **Fig. 2**). It is based on a scanning probe microscopy software, which requires low computational power and, therefore, is suitable for routine bedside use. Both surface and vascular structures can be separately recorded and digitally traced in an endoscopic image in real time. These marked structures can be displayed as an adjunct to the endoscopic image on a second monitor, or as a picture-in-picture, clearly visualizing these complex structures. Surface pattern (SP) and vascular pattern (VP) of lesions are visualized and, in a second step, quantified with respect to irregularity and other morphological descriptive properties. These results are subject to statistical comparison with normal findings.

In the context of colorectal lesions, BEE variables reflect the irregularity and density of VP and SP, which are essential criteria for JNET classification.

In the present pilot study, still images of LCL were analyzed retrospectively with BEE, and the collected variables directly compared to the histology of the resected specimens.

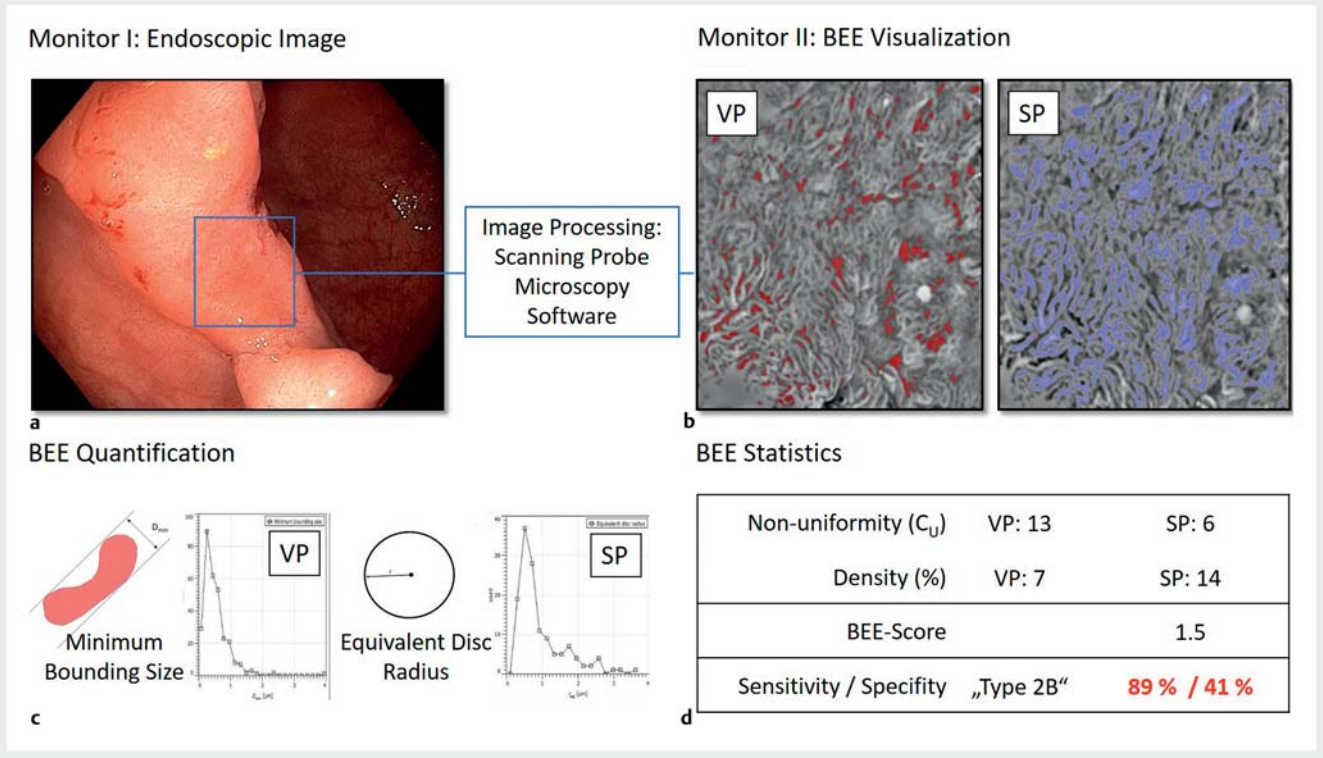

▶ **Fig. 2** Bioinformatically enhanced endoscopy (BEE): optical and mathematical analysis of microsurface (SP) and vascular (VP) patterns on the routine endoscopic white-light HD image. **a** After marking the suspect area on the frozen endoscopic image, **b** SP and VP are simultaneously traced by the software in real time on a second monitor for enhanced perceptibility. VP and SP are also quantified. **c** Here, the equivalent circular radii of SP, and caliber diameters of VP are calculated. **d** In the last step, an index for irregularity is calculated and mathematically evaluated: nonuniformity coefficient (C_U) as the slope of a cumulative frequency distribution curve of the equivalent circular radii of SP or of caliber diameters of VP, respectively. Density is defined as the proportion of the area of labeled VP and SP structures to the total area. These BEE variables allow calculation of the BEE-score and consecutive statistical evaluation.

Patients and methods

HD-WLE images of 26 LCLs from 26 patients treated at our center from January 1, 2018 to December 31, 2019 were retrospectively analyzed withy BEE. We included only lesions for which optimal optical documentation (all parts of the lesion clearly visible, HD quality) was available. The initial endoscopic optical classification of the lesions before resection was not taken into account. For statistical comparison, the lesions were categorized by histology in clinical relevant subgroups according to the JNET classification [4, 5]. These categories are referred to as Type 2A for adenomas with low-grade intraepithelial neoplasia (LGIN, n = 10), Type 2B for high-grade intraepithelial neoplasia (HGIN) or early carcinoma (n = 9) (EAC), and Type 3 for invasive carcinomas (≥ T1sm2, n = 7) in the text. The mean diameter of the lesions was 39 mm. The characteristics of the patients and lesions are summarized in ▶ **Table 1**. Becaue of the retrospective and noninvasive character of the study, the Ethics Committee waived the issue of a statement.

For the BEE process, we use free, open-source software, covered by a GNU General Public License, which can process data on height fields usually obtained with scanning probe microscopy (gwyddion.net) [7]. In the context of BEE, the software is used for image processing of HD-WLE images. Grain analysis is accomplished by thresholding algorithms after background subtraction and filtering. For SP and VP, best results could be achieved with grain analysis after measurement of intensity, intensity slope, und intensity curvature. In our set of lesions, we used two groups of variables, focusing on density and irregularity of vascular (VP) and surface structures (SP), respectively, because all clinical classifications are based on these key issues.

The measure for irregularity was inspired by soil mechanics, grain size analysis, gradation, and sieve curve terminology [8]. For irregularity analysis of surface structures, distributions of area-related grain properties, the equivalent disc radii (radius of the disc with the same projected area as the grain) were calculated. For irregularity analysis of vascular structures, distributions of boundary-related grain properties, the minimum bounding sizes (minimum dimension of the grain in the horizontal plane) were estimated (▶ **Fig. 3**). BEE variables were defined as follows: density as the proportion of the labeled area of VP and SP structures in relation to the total area. Nonuniformity coefficient (C_U) as the slope of a cumulative frequency distribution curve of the equivalent circular radii of SP or of caliber diameters of VP, respectively. To better characterize different histological subgroups, we computed a complex variable (BEE score). After preliminary theoretical considerations, a specific BEE variable constellation was defined, based on established

▶ **Table 1** Baseline characteristics of included patients and lesions.

Patient no.	Age	Sex	Localization	Diameter (mm)	Type of resection	Morphology	Histology
Subgroup Type 2A							
1	83	M	l Fl	40	PM-EMR	gm	t.-v., LGIN
2	91	M	Asc	23	EMR en-bl	Is	tub., LGIN
3	58	F	Rectum	25	EMR en-bl	gm	t.-v., LGIN
4	72	F	Cecum	30	PM-EMR	gm	t.-v., LGIN
5	72	M	Asc	35	ESD	gm	tub., LGIN
6	71	M	Asc	35	ESD	gm	t.-v., LGIN
7	91	M	Asc	25	EMR en-bl	gm	tub., LGIN
8	73	M	Transv	25	EMR en-bl	gm	tub., LGIN
9	76	F	Cecum	25	PM-EMR	gm	t.-v., LGIN
11	56	F	Rectum	35	PM-EMR	gm	t.-v., LGIN
Subgroup Type 2B							
10	70	F	Rectum	70	ESD	gm	t.-v., HGIN, pTis
12	83	F	Cecum	45	PM-EMR	gm depr	G2 sm1
13	72	F	Asc	30	PM-EMR	gm	tub., HGIN
14	81	F	Asc	25	EMR en-bl	gm	tub., HGIN
15	83	F	Rectum	40	ESD	gm	t.-v., HGIN
16	83	M	Sigmoid	25	PM-EMR	Is depr	tub., HGIN
17	58	F	Sigmoid	40	ESD	gm	tub., HGIN
18	62	M	Transv	25	ESD	gm depr	G2, pTis (m3)
19	79	F	Cecum	35	ESD	gm	G2 sm1
Subgroup Type 3							
20	70	M	Rectum	30	FTR	NGPD	T2
21	50	F	Rectum	80	OP	gm depr	T2
22	77	M	Asc	40	OP	NGPD	T2
23	83	M	Asc	70	OP	NGPD	T2
24	75	F	Cecum	50	OP	Is depr	G2 sm2
25	47	F	Rectum	50	OP	gm depr	T3
26	75	F	Sigmoid	50	OP	gm depr	T2
Mean	72.7			38.6			
95 % CI	[68.3, 77.2]			[32.7, 44.5]			

LGIN, low-grade intraepithelial neoplasia; Fl, left flexure; Asc, colon ascendens; Transv, colon transversum; EMR, endoscopic mucosal resection; PM-EMR, piecemeal EMR; EMR en-bl, en-bloc EMR; ESD, endoscopic submucosal dissection; FTR, full thickness resection; gm: lateral spreading tumor granular mixed type; Is: Paris-Japanese Type O-Is; depr: depressed; NGPD: lateral spreading tumor non granular pseudodepressed type.

endoscopic classifications in colorectal cancer [2, 3]. BEE score was defined as the combined products of density and reciprocal irregularity of SP and VP. Due to high densities of SP and VP and low irregularity indices, a high BEE score value should represent a low probability of malignancy.

$$BEE - Score = \frac{Density\ VP * Density\ SP}{C_U VP * C_U SP}$$

BEE variables and BEE scores for SP and VP were evaluated and statistically compared to histology from endoscopic resection or surgery. Two-factor analysis of variance for Friedman ranks in related samples and Spearman correlation coefficient for univariate non-parametric testing and receptor operating characteristics (ROC) analysis for sensitivity, specificity, and optimal threshold value were used (IBM SPSS Statistics, Version

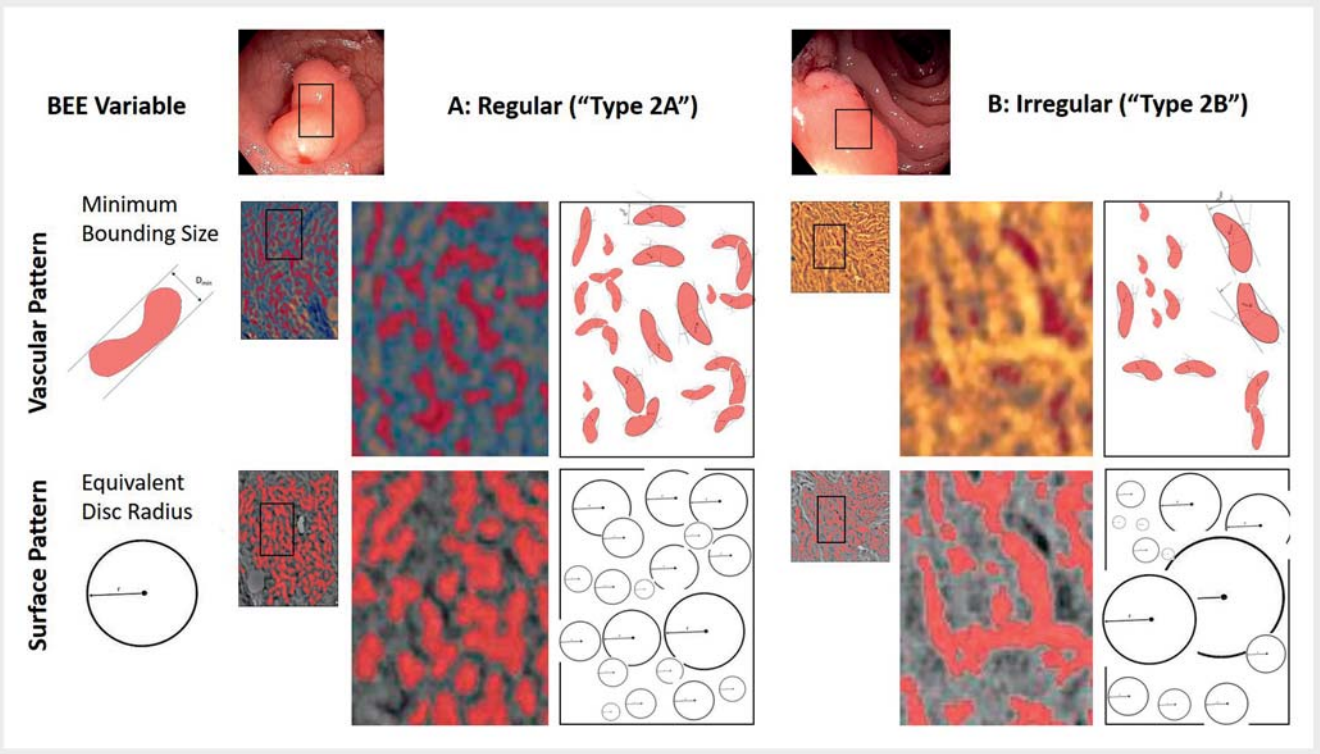

▶ **Fig. 3** Bioinformatically enhanced endoscopy (BEE): mathematical analysis of microsurface (SP) and vascular (VP) patterns based on grain analysis after height, slope and curvature thresholding. For irregularity analysis of surface structures, distributions of area-related grain properties, the equivalent disc radii (radius of the disc with the same projected area as the grain) were calculated. For irregularity analysis of vascular structures, distributions of boundary-related grain properties, the minimum bounding sizes (minimum dimension of the grain in the horizontal plane) were calculated. These BEE variables allowed calculation of the BEE-score and consecutive statistical evaluation. Here, regular (**a**, adenoma with low-grade intraepithelial neoplasia) and irregular vascular and surface patterns of two lesions (**b**, adenoma with high-grade intraepithelial neoplasia) are compared, respectively.

27). $P<0.05$ was considered statistically significant. The optimal threshold value was the test value for which the hit rate (sensitivity) and rate of correct rejections (specificity) were maximized in total using the Youden Index (sensitivity + specificity-1).

Results

The visual and statistical matrix of the BEE analysis is summarized in ▶ **Fig. 4**. Depending on histology and degree of invasion, the BEE score changed significantly (Friedman test, $P<0.05$). The density of marked VP and SP structures, as well as the slope of a cumulative frequency distribution curve (C_U, nonuniformity) of the equivalent circular radii of SP and of caliber diameters of VP, respectively, correlated with histological subclassification. Sensitivity and specificity were calculated with the highest results for the BEE score. ROC analysis revealed optimal thresholds for the BEE score when a threshold value of 3.6 had been chosen, the sensitivity to characterize a (benign) subgroup Type2A was 90 %. When a threshold value of <0.5 had been chosen, the sensitivity for characterizing an invasive subgroup Type 3 was 100 %. The measured and computed BEE variables are summarized in ▶ **Table 2** and Supplemental Figures for all lesions.

Discussion

The aim of this pilot study was to reduce interobserver variance with BEE. We used a well-defined set of WLE still images with corresponding histopathology (as gold standard) to test whether specific size and form distributions coincided with one of the histologic categories. The results of the present pilot study suggest that BEE is a feasible tool for enhancing visual representation of microsurface (SP) and vascular (VP) patterns. In addition, quantification and statistical analysis of the density and irregularity of these variables showed significant results in assessment of LCLs. Only two lesions were misclassified: the lesion in Patient 19 was classified by BEE scoring as Type 3 due to a relatively low density of VP and SP. Histology after endoscopic submucosal dissection revealed adenocarcinoma G2Tsm1. The lesion in Patient 9 was classified by BEE scoring as Type 2B, showing a low density of VP. It was difficult to evaluate the VP in this case because of presence of a an opaque white substance. Histology revealed a tubulovillous adenoma with LGIN. However, positive predictive values for BEE scoring were 100 %, and 87 % for the histological subgroups Type 2A and Type 3, respectively.

Lesions with HGIN or EAC (Type 2B) presented with a high density of vascular and surface structures, and mainly irregular-

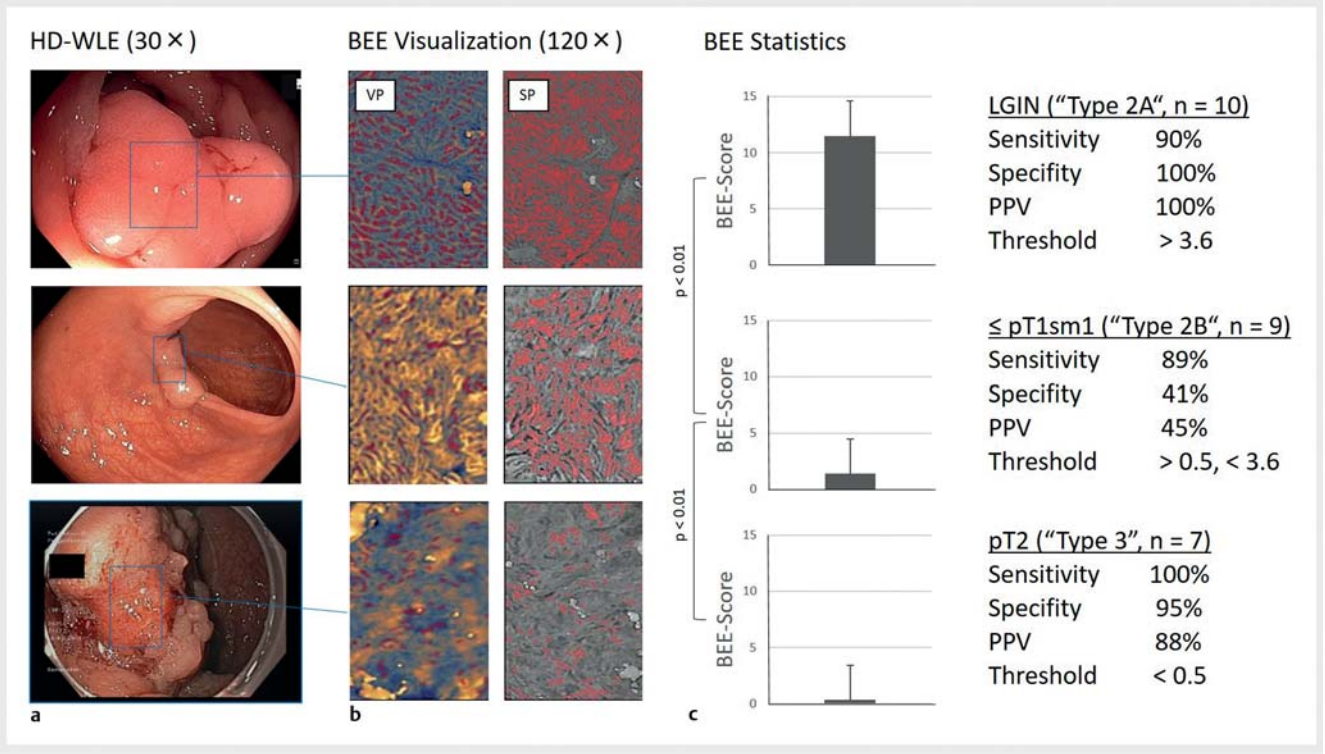

▶ **Fig. 4** Visual and statistical evaluation of BEE variables of SP and VP. Depending on the degree of invasion and histological classification, the BEE-score changes significantly (Friedman test, $P<0.05$). Sensitivity, specificity and optimal threshold values were derived from BEE-score by receptor-operating-characteristics analysis. HD-WLE, white-light endoscopy in HD; SP, microsurface pattern; VP, microvascular pattern; LGIN, low-grade intraepithelial neoplasia; PPV, positive predictive value.

ity aspects were responsible for the differentiation from benign lesions. This could explain the limited sensitivity and specificity of the BEE score in the subgroup Type 2B. The BEE score could be optimized in these cases by factor analysis, which we omitted because of the small size of the actual pilot trial.

Another positive effect of BEE is visualization of microstructures, providing feedback to the endoscopist. Separate visualization of SP and VP facilitates correct classification, visually and mathematically. Thus, examiners learn to focus on meaningful endoscopic images. BEE is based on SP and VP, as established by Japanese experts and supported by clinical evidence [4,5]. Therefore, there is no need to establish a new (confusing) classification for BEE analysis. However, especially in large lesions and for unexperienced endoscopists, selection of a particular area of interest for BEE analysis may be difficult, leading to risk of misclassification.

Furthermore, BEE also could be applied to other parts of the gastrointestinal tract. In those areas, other classifications, such as the vessel plus surface classification in the stomach, or the JES classification in the esophagus [1], could be used as a reference.

In contrast to applications from the field of deep learning and artificial intelligence, BEE requires only minimal computing power, and no pre-training procedures. Visualization and calculations for density and nonuniformity are performed in fractions of a second. The traced complex structures can be perceived more intensively with respect to their irregularity. They can be quantified and statistically compared with normal findings. This analysis could complement routine diagnostic procedures such as virtual and real chromoendoscopy to improve diagnostic accuracy (especially by reducing interobserver variability). The accuracy of BEE scoring may be improved by factor analysis in future statistical evaluations in the context of a large clinical evaluation. This process could be integrated into the device software and applied directly during examination. Such a process has not yet been reported or attempted.

This small pilot study has several limitations. We included six lesions with LGIN and HGIN and one EAC sm1, which were resected in piecemeal fashion. However, in all these cases, histology could clearly evaluate basal extension, invasion depth, lymphovascular invasion, and grading. Furthermore, the very small sample size did not allow strong conclusions and statistic evaluation was limited. To improve quantitative BEE diagnostics, factor analysis and development of a prediction model should be derived from a validation set of lesions and prospectively tested in a large cohort of patients.

Conclusions

We conclude that BEE, if implemented in real time, could support assessment of LCLs in routine endoscopy and underpin treatment decisions. However, the present small case series has only limited validity. Therefore, prospective controlled clinical trials and further technical solutions, such as automation

▶ **Table 2** BEE variables and statistical analysis.

	Density VP (%, [95 % CI])		Density SP (%, [95 % CI])		C_U SP [95 % CI]		C_U VP [95 % CI]		BEE- score [95 % CI]	
Subgroup Type 2A, n = 10										
Mean	14.8	[11.0, 19.2]	28.4	[22.3, 32.7]	6.4	[4.9, 7.5]	9.0	[7.8, 10.8]	9.8	[4.4, 14.1]
Sensitivity	90	[47, 81]	69	[52, 82]	70	[53, 90]	70	[48, 83]	90	[71, 93]
Specifity	88	[56, 91]	69	[54, 81]	81	[38, 71]	69	[33, 68]	100	[54, 80]
PPV	82	[64, 90]	66	[58, 74]	70	[45, 56]	58	[44, 61]	100	[64, 82]
Threshold value	8.5	[7.9, 15.9]	17.5	[15.6, 25.8]	6.9	[7,5, 13,1]	9.5	[9.0, 14.4]	3.6	[3.0, 10.5]
Subgroup Type 2B, n = 9										
Mean	7.1	[5.8, 8.2]	19.6	[14.6, 25.2]	10.1	[8.3, 13.3]	13.2	[9.6, 16.8]	1.2	[0.2, 3.4]
Sensitivity	89	[12, 54]	89	[30, 62]	67	[37, 71]	89	[45, 80]	89	[29, 61]
Specifity	35	[40, 69]	41	[42, 67]	71	[44, 77]	65	[47, 83]	41	[35, 54]
PPV	43	[7, 25]	45	[24, 35]	55	[36, 52]	58	[53, 79]	45	[15, 28]
Threshold value	5.5	[7.9, 15.9]	11.0	[15.6, 25.8]	9.0	[7.5, 13.1]	9.5	[9.0, 14.4]	0.5	[1.6, 5.9]
Subgroup Type 3, n = 7										
Mean	4.1	[1.9, 6.3]	6.6	[4.4, 8.7]	11.1	[6.6, 15.5]	9.1	[7.6, 10.7]	0.3	[0.2, 0.4]
Sensitivity	86	[66, 96]	100	[73, 99]	86	[39, 70]	43	[45, 84]	100	[70, 94]
Specifity	79	[31, 67]	95	[52, 72]	47	[42, 76]	79	[31, 65]	95	[52, 77]
PPV	40	[40, 65]	87	[43, 64]	38	[32, 52]	43	[25, 35]	88	[49, 67]
Threshold value	6.5	[7.9, 15.9]	11.0	[15.6, 25.8]	6.9	[7.5, 13.1]	8.4	[9.0, 14.4]	0.5	[1.6, 5.9]
Analysis of variance, p[1]	0.01		0.01		0.01		0.01		0.04	
Correlation (p)[2]	-0.77 (<0.01)		-0.76 (<0.01)		0.45 (0.02)		0.13 (0.52)		-0.90 (<0.01)	

SP, microsurface pattern; VP, microvascular pattern; C_U, nonuniformity; LGIN, low-grade intraepithelial neoplasia; SEM, standard error of the mean; PPV, positive predictive value.
[1] Friedman test
[2] Spearman correlation

and integration of the BEE algorithm into the processor software of endoscopy systems, are required.

Acknowledgments

The authors are particularly grateful for the valuable and constructive suggestions from Dr. Christoph Schendel and Alexander Wagner during the planning and development of this research work.

Competing interests

The authors declare that they have no conflict of interest.

References

[1] Wagner A, Zandanell S, Kiesslich T et al. Systematic Review on Optical Diagnosis of Early Gastrointestinal Neoplasia. J Clin Med 2021; 10: doi:10.3390/jcm10132794

[2] Backes Y, Moss A, Reitsma JB et al. Narrow band imaging, magnifying chromoendoscopy, and gross morphological features for the optical diagnosis of T1 colorectal cancer and deep submucosal invasion: a systematic review and meta-analysis. Am J Gastroenterol 2017; 112: 54–64

[3] Wagner A, Maehata T, Berr F et al. Colorectum: Mucosal Neoplasias. In: Berr F, Oyama T, Ponchon T et al. Atlas of Early Neoplasias of the Gastrointestinal Tract: Endoscopic Diagnosis and Therapeutic Decisions. 2nd edn. Springer; 2019: 318

[4] Iwatate M, Sano Y, Tanaka S et al. Validation study for development of the Japan NBI Expert Team classification of colorectal lesions. Dig Endosc 2018; 30: 642–651

[5] Sano Y, Tanaka S, Kudo SE et al. Narrow-band imaging (NBI) magnifying endoscopic classification of colorectal tumors proposed by the Japan NBI Expert Team. Dig Endosc 2016; 28: 526–533

[6] Vleugels JLA, Koens L, Dijkgraaf MGW et al. Suboptimal endoscopic cancer recognition in colorectal lesions in a national bowel screening programme. Gut 2020; 69: 977–980

[7] Necas D, Klapetek P. Synthetic data in quantitative scanning probe microscopy. Nanomaterials 2021; 11: doi:10.3390/nano11071746

[8] Gee GW, Or D. Particle-Size Analysis. In: Dane JH, Topp CG. Methods of Soil Analysis, Part 4: Physical Methods. John Wiley & Sons; 2020: 1744